Adsorption (2007) 13: 477–484
DOI 10.1007/s10450-007-9031-7

Monte Carlo and energy minimization studies of binary xylene adsorption in AEL and AFI networks

S. Mardônio P. Lucena · Randall Q. Snurr · Célio L. Cavalcante Jr.

Received: 29 April 2007 / Revised: 13 July 2007 / Accepted: 23 July 2007 / Published online: 20 September 2007

Abstract Adsorption of binary xylene mixtures in AEL and AFI networks was investigated using normal and biased GCMC simulations. Preferential *o*-xylene adsorption was evidenced in the simulations, as previously reported in single-component experimental data. In contrast to the FAU and MFI sieves, the AEL and AFI networks exhibit surprising azeotropic behavior. The selectivity switches from *o*-xylene to *p*-xylene at a gas phase mole fraction of ca. 0.5. Energy minimization was performed in the $AlPO_4$-11 molecular sieve to determine the energy differences between the adsorption sites. The minimization study showed that $AlPO_4$-11 has small adsorption energy differences between sites. The azeotropic behavior of the AEL and AFI networks can be explained using the two patch model proposed by Do and Do (Adsorption 5:319–329, 1999).

Keywords Aluminophosphate · Xylenes · Simulation · Monte Carlo · Sorption · Binary

1 Introduction

In the petrochemical industry, the separation of xylenes is the main application of adsorption separations. The current process of separating *p*-xylene from C_8 aromatic mixtures is performed by taking advantage of the *para*-selective adsorption behavior of the FAU type zeolite (Buarque et al. 2005; Minceva and Rodrigues 2004).

Ortho-selectivity in aluminophosphate molecular sieves was identified experimentally for xylene adsorption in AFI ($AlPO_4$-5) (Barthomeuf and De Mallmann 1990; Chiang et al. 1991) and AEL ($AlPO_4$-11) (Cavalcante et al. 2000). Those experimental studies were done with pure components. The only experimental work with multicomponent mixture was done by Rosenfeld and Barthomeuf (1983).

The need to gain a detailed insight into the behavior of molecular sieve/sorbate systems on the molecular scale motivated us to perform molecular simulation studies of single components using the grand canonical Monte Carlo (GCMC) technique. We found for example that the selectivity in AFI and AET networks is due to the characteristic *o*-xylene face-to-face positioning, which allows more efficient packing within the pores (Lucena et al. 2006a, 2006b). On the other hand, AEL *ortho*-selectivity comes from the smaller length of the *o*-xylene molecules in the c-axis direction compared to *p*-xylene. We also found that channel modulation, creating wide and narrow regions along the aluminophosphate channels, is a decisive factor for the adsorption properties of xylenes.

Considering that the exact coadsorption isotherm can be obtained directly from GCMC simulations of a mixture, in this work we extend our previous studies to multicomponent systems. The direct mixture simulation can give information about the differences between the single and the multicomponent adsorbed phases. Such information will be very helpful to broaden the understanding of molecular selectivity.

Lachet et al. (1998, 1999, 2001) and Mohanty et al. (2000) reported molecular simulations of xylene mixture adsorption from the gaseous phase in KY and silicalite, respectively. Chempath et al. (2004) used GCMC simulations to

S.M.P. Lucena · C.L. Cavalcante Jr. (✉)
Universidade Federal do Ceará, Dept. Eng. Química, Grupo de Pesquisa em Separações por Adsorção—GPSA, Campus do Pici, Bl. 709, 60455-760 Fortaleza, CE, Brazil
e-mail: celio@gpsa.ufc.br

R.Q. Snurr
Northwestern University, Department of Chemical & Biological Engineering, Evanston, IL 60208, USA

predict adsorption of aromatic mixtures in silicalite from the liquid phase and found good agreement with experimental binary adsorption data from the literature. In all these studies, selectivity of *p*-xylene occurs within all molar fractions of *p*-xylene range in the mixture.

In the following sections we present binary mixture isotherms for *o*- and *p*-xylene at three different gas-phase compositions in the AFI and AEL frameworks. The isotherms were calculated using GCMC and a new force field fitted for *o*-xylene in $AlPO_4$-5 from our previous study (Lucena et al. 2006a). Structural analysis, adsorption energy data and experimental results are used to clarify the selectivity behavior of the mixtures. Energy minimization calculations were performed in the $AlPO_4$-11 adsorption sites to help evaluating any interaction energy difference. We show that the two patch model for adsorption of binary mixtures proposed by Do and Do (1999) can explain the azeotropic behavior of these systems.

2 Simulation model

2.1 Sorbate-sorbate interaction

The xylene molecules were treated using an all-atom representation (AA model), and the xylene-xylene interactions were modeled with a Lennard-Jones (LJ) potential between all pairs of atomic centers. For the normal and energy biased GCMC studies, the interaction parameters were taken from Jorgensen et al. (1993). We have changed the methyl united atom model of Jorgensen et al. to an AA model. The carbons and hydrogens in the methyl groups were treated the same as those in the aromatic rings. From our previous study (Lucena et al. 2006b) it was observed that sorbate-sorbate interactions had only a minor effect on the system behavior, thus the Coulomb interactions between xylene molecules were not considered. The potential parameters are listed in Table 1. The cross terms were obtained using arithmetic and geometric combination rules.

2.2 Sorbate-aluminophosphate interaction

In these systems, the xylene molecules were assumed to interact only with the oxygen atoms of the molecular sieve framework. The interactions with Al and P atoms were ignored as previously done by other authors (Kiselev et al. 1985). The dispersion and repulsion forces between xylene and aluminophosphate atoms were modeled using Lennard-Jones potentials. For the normal and energy biased GCMC studies we took the LJ potentials between C and H and the framework oxygen atoms from Bhide and Yashonath (2000). Previously, we adjusted the carbon LJ parameters in the methyl group so that the xylene-aluminophosphate interaction energy is close to the low loading adsorption heat value

Table 1 LJ dispersion-repulsion parameters used in the calculations of xylene-xylene and xylene-aluminophosphates interactions (C3 is the carbon in the methyl group)

	C[a]	H[a]	C–O[b]	H–O[b]	C3–O
σ (Å)	3.55	2.42	2.99	2.71	3.02
ε (kcal mol^{-1})	0.07	0.03	0.254	0.068	0.185

[a]From Jorgensen et al. (1993)

[b]From Bhide and Yashonath (2000)

observed experimentally for *o*-xylene in $AlPO_4$-5 (Chiang et al. 1991). The values for these parameters are also given in Table 1. No Coulomb interactions have been included between the xylenes and aluminophosphates. This can be justified because in neutral zeolitic structures, such as silicalite, the contribution of the electrostatic forces in high occupancy aromatic adsorption is only about 5–14% of the total value of the adsorption heat (Clark and Snurr 1999).

2.3 Structural details

The xylene molecules were considered planar and rigid in the GCMC simulations. The structures of the molecular sieves $AlPO_4$-5 and $AlPO_4$-11 were taken from Bennett et al. (1983, 1987). $AlPO_4$-5 crystallizes in the space group P6/mcc (a = 13.8 Å and c = 8.45 Å) with 72 atoms/unit cell. It forms one-dimensional pores with free diameter of 7.3 Å parallel to the crystallographic c direction (AFI structural network—hexagonal). $AlPO_4$-11 crystallizes in the space group Imma (a = 13.534 Å, b = 18.482 Å, c = 8.370 Å) with 120 atoms/unit cell. It forms one-dimensional pores with free diameter of 6.5 × 4.0 Å parallel to the crystallographic c direction (AEL structural network—orthorhombic).

In aluminophosphates, the channels do not have uniform diameter. They exhibit a diameter modulation along the c axis, leading to alternate wide and narrow cross sections. The narrow region, or window, is the ring of oxygen atoms, and the wide region corresponds to the area of connections between two windows (see Fig. 1). $AlPO_4$-5 has narrow windows with 12 oxygen atoms with diameter of 9.96 Å and wide regions (connecting two consecutive windows) with diameter of 11.20 Å (see Fig. 1A). $AlPO_4$-11 has windows with 10 oxygen atoms with diameters of 9.31 × 7.06 Å and wide regions with diameters of 10.40 × 7.80 Å (see Fig. 1B). We have shown (Lucena et al. 2006a) that these pore variations and the corresponding interaction energy of the molecule–crystal lattice drive all molecular positioning. The *ortho*-selectivity depends mainly on how this modulation influences the fitting of the molecules.

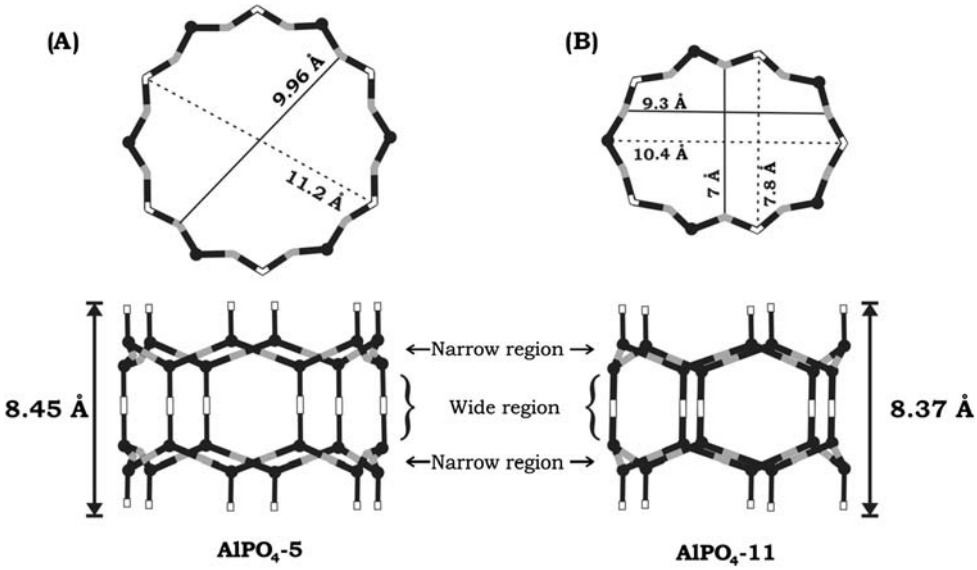

Fig. 1 Cross-sectional and side view of the channels of $AlPO_4$-5 (AFI) and $AlPO_4$-11 (AEL). (**A**) There are two diameters in the cross-sectional view of $AlPO_4$-5, the narrow (9.96 Å) and the wide (11.20 Å). In the side view we can see the different regions indicated along the channel. (**B**) There are two diameters in the cross-sectional view of $AlPO_4$-11: the narrow (9.3 × 7.0 Å) and the wide (10.4 × 7.8 Å). Diameters are taken between the centers of the oxygen atoms of the narrow and wide regions. Aluminum and phosphorus atoms: *black balls*; oxygen atoms in the windows: *gray bars*; oxygen atoms in the wide regions: *white bars*. Cross-sectional views represent one wide and one narrow section

2.4 Computational details

The calculations of the binary isotherms were performed in a simulation cell containing 27 unit cells (3 × 3 × 3). Monte Carlo simulations in the grand canonical ensemble were carried out using the standard procedure (Frenkel and Smit 2002). This involves creation and destruction of molecules which interact with the potential field generated by the atoms comprising the aluminophosphate lattice, which is assumed to be rigid. Equilibrium is achieved when the chemical potential of the gas inside the framework is equal to the chemical potential of the free gas outside the framework. At the low pressure conditions considered here, the chemical potential was calculated from the gas pressure and temperature assuming that the external bulk gas is ideal. Partial pressures were used in the case of multi-component gas mixtures.

The AFI network was treated with conventional GCMC technique. However, AEL network has smaller pores than AFI. It is known that in systems where molecules are adsorbed in very restricted spaces, conventional GCMC simulations have difficulties in sampling the configurational states. Then, an energy biased GCMC technique was used in the adsorption isotherm simulations of AEL network. In this scheme, insertions are biased so that they are attempted more often in the energetically more favorable regions of the sieve. Method details can be seen elsewhere (Snurr et al. 1993). The conventional GCMC simulations have been performed in a SGI Onyx2 station using Cerius2 software suite (Sorption 2001). The energy biased GCMC simulations were performed on a PC Intel Pentium 4, 3.0 GHz processor, using the MUSIC code (Gupta et al. 2003). Between 3 and 5×10^6 Monte Carlo steps were performed in order to calculate mean values. The potential cut-off distance was 12 Å, with a low cutoff of 0.4 Å. Each run lasted from two to four hours of computing time.

The simulation cell used in the energy minimization study was loaded with one xylene molecule using a canonical ensemble Monte Carlo algorithm (fixed loading). The energy minimization method was supplied by the same cited Cerius2 software suite. We used the Burchart force field (Vos Burchart et al. 1992) for the molecular sieve and the UFF force field (Rappé et al. 1992) for the molecules. In the minimization, the framework was also assumed to be rigid and the atoms of the sorbate molecules were flexible.

3 Results and discussion

3.1 Adsorption of binary mixtures

The calculated adsorption isotherms of pure *o*- and *p*-xylene at 30 °C for $AlPO_4$-5 and at 60 °C for $AlPO_4$-11 are shown in Fig. 2. In the same figure we can see the simulated adsorption isotherm for binary mixtures containing 20, 50 and 80% *p*-xylene.

As previously seen for the pure component isotherm, the adsorbed phase concentration of the mixtures reaches about 80% of the total sorption capacity still at very low pressure ($P/P_o < 0.03$).

The total amount of adsorbed *o*- plus *p*-xylene per unit cell, as expected, are located between the two curves of pure components over the whole pressure range. Similar results were found by Lachet et al. (1999) for xylenes mixtures in NaY and KY.

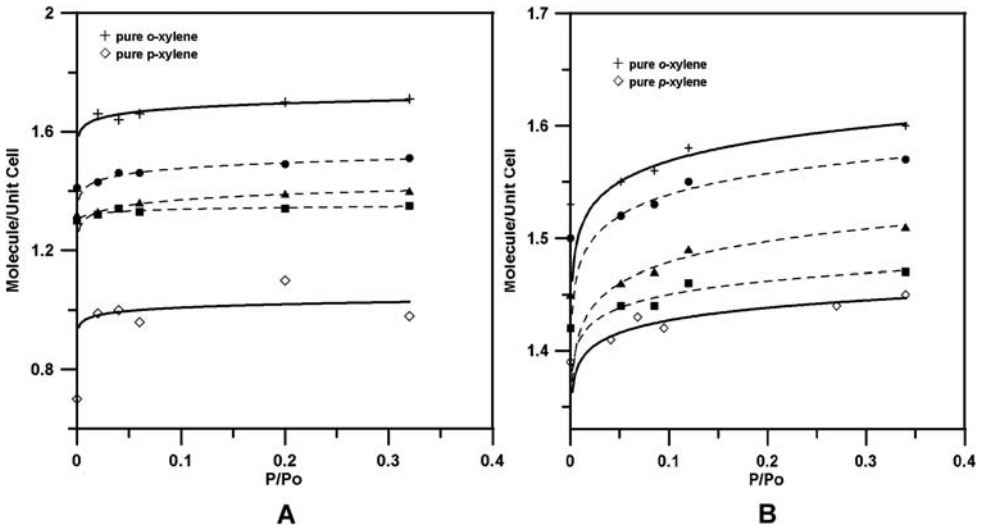

Fig. 2 Adsorption isotherms for pure and binary mixture of xylenes in $AlPO_4$-5 at 30 °C (**A**) and $AlPO_4$-11 at 60 °C (**B**). Pure species (*filled lines* and *open symbols*). Binary mixtures (*dashed lines* and *filled symbols*): 20% *p*-xylene-80% *o*-xylene (*circle*), 50% *p*-xylene-50% *o*-xylene (*triangle*) and 80% *p*-xylene-20% *o*-xylene (*square*)

For $AlPO_4$-5, the pure component maximum loading is 1.7 (*o*-xylene) and 0.98 (*p*-xylene) molecules/unit cell. These values can be compared with the experimental data of Chiang et al. (1991) in the same temperature. The binary mixture 20% *p*-xylene-80% *o*-xylene has the highest saturation loading of the three tested gas-phase compositions with 1.51 molecules/unit cell. The mixture 80% *p*-xylene-20% *o*-xylene has the lowest saturation loading with 1.35 molecules/unit cell.

The $AlPO_4$-11 molecular sieve presented similar results. The pure component loading range was 1.6 and 1.45 molecule/unit cell for *o*- and *p*-xylene respectively. The binary mixture 20% *p*-xylene-80% *o*-xylene has the highest saturation loading with 1.57 molecules/unit cell and the mixture 80% *p*-xylene-20% *o*-xylene has the lowest saturation loading with 1.47 molecules/unit cell.

Adsorption heats were calculated during the simulation for different loadings. In Fig. 3 we can see the results for the $AlPO_4$-5 sieve.

In $AlPO_4$-5, the simulated low coverage adsorption heat for *o*- and *p*-xylene is equal to 18 kcal/mol and 16.8 kcal/mol respectively. It is interesting to remember that we adjusted the carbon LJ parameters in the methyl group so that the xylene-aluminophosphate interaction energy is close to the low loading adsorption heat value observed experimentally for *o*-xylene (17.6 kcal/mol) (Chiang et al. 1991). Figure 3 shows that up to a loading of approximately 1 molecule/unit cell the value of the adsorption heat increases slowly for both *o*- and *p*-xylene. Over 1 molecule/unit cell the value of the adsorption heat of *o*-xylene increases substantially. This is due to the particular face-to-face positioning of o-xylene adsorbed in $AlPO_4$-5 as previously reported for this system (Lucena et al. 2006b). On the other hand, *p*-xylene saturates at 1 molecule/unit cell, without further adsorption (the dashed line in Fig. 3 is only for eye guide).

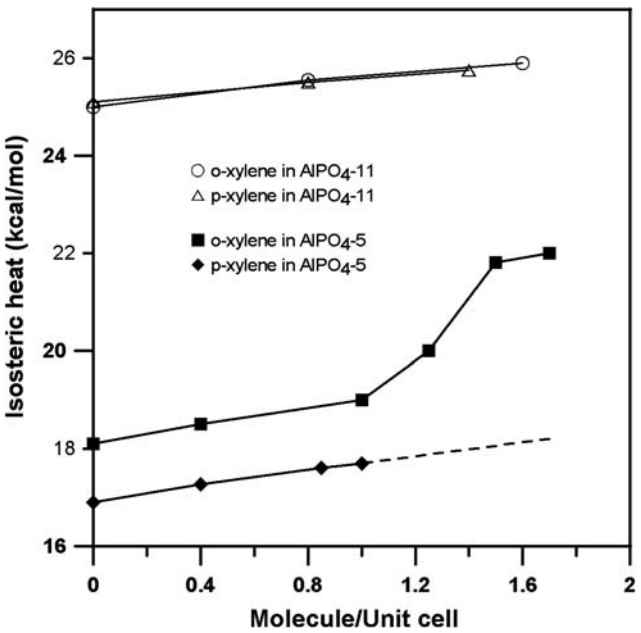

Fig. 3 Variation of adsorption heat with loading for pure *p*- and *o*-xylene in $AlPO_4$-5 at 30 °C and $AlPO_4$-11 at 60 °C

Due to the large relative ratio between the molecule size of xylenes and the pore size of $AlPO_4$-5, the *p*- and *o*-xylene molecules perceive each of the aluminophosphate adsorption sites as almost energetically uniform (Ruthven 1984). The sorbate-sieve interaction energy is almost invariable. The increment of the energy with concentration observed in the data shown in Fig. 3 comes exclusively from the sorbate-sorbate interaction.

For $AlPO_4$-11, the adsorption heats of *o*- and *p*-xylene are almost the same. The simulated low coverage adsorption heats for the two species is ca. 25 kcal/mol and this value changes only about 1 kcal/mol in the high coverage range (see Fig. 3). We note that the molecule-molecule interac-

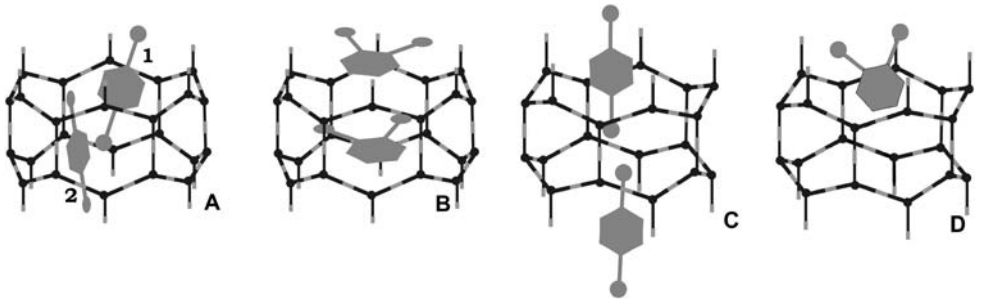

Fig. 4 Schematic representation of *p*-xylene (**A**), *o*-xylene (**B**) in $AlPO_4$-5 channels at 30 °C and *p*-xylene (**C**), *o*-xylene (**D**) in $AlPO_4$-11 channels at 60 °C. (**A**) molecules of *p*-xylene are positioned preferentially in the narrow window (*1*) and can be also adsorbed in the wide region (*2*); (**B**) molecules of *o*-xylene are always disposed face-to-face in the wide region; (**C**) molecules of *p*-xylene are positioned in the wide region; (**D**) molecules of *o*-xylene are positioned only in the narrow windows

tion energy between *o*-xylene is double of that for *p*-xylene molecules (due to steric reasons, because *o*-xylene molecules can pack more tightly than *p*-xylene molecules inside the $AlPO_4$-11 pore). All molecule–molecule interaction energy represents only 3% of the total interaction energy of the system.

In previous single components molecular simulation studies (Lucena et al. 2006b) we characterized the location of the adsorbed molecules in the aluminophosphate molecular sieves. In both molecular sieves, the xylene isomers are found to be adsorbed in two different sites. In $AlPO_4$-5, the *o*-xylene molecules adsorb in the pore wide region in a face-to-face position. The *p*-xylene isomer adsorbs preferentially in the narrow windows and some adsorption also occurs in the wide regions (see Fig. 4). In $AlPO_4$-11, *o*-xylene adsorbs in the narrow windows parallel to the pore wall. The *p*-xylene molecules adsorbs in the wide region (see Fig. 4). We can note from the statistics of mass center location, that $AlPO_4$-11 *p*-xylene molecules are more delocalized around the adsorption sites than the *o*-xylene ones. In the binary simulations, both *o*- and *p*-xylene isomers still exhibit the same site locations that had been observed for the simulations with single components.

3.2 Mixture adsorption selectivity

The adsorption selectivity for *p*-xylene ($\alpha_{px/ox}$) is calculated using the equation:

$$\alpha_{px/ox} = \frac{X_{px}}{Xox} \times \frac{Yox}{Ypx} \tag{1}$$

where X_i and Y_i are the molar fractions of component i in the adsorbed phase and in the gas phase, respectively. A value of $\alpha_{px/ox}$ different from unity means that selectivity is observed. If the value is greater than 1, the molecular sieve is *p*-selective and for values lower than 1 the system is *o*-selective. The calculated adsorption selectivities are shown in Table 2.

Table 2 Calculated adsorption selectivities

	$\alpha_{px/ox}$		
	20% px-80% ox	50% px-50% ox	80% px-20% ox
$AlPO_4$-5	1.3	0.67	0.24
$AlPO_4$-11	3.4	1.0	0.28

Azeotropic behaviour ($\alpha_{px/ox} > 1$) is observed at *p*-xylene gas phase mol fractions under 37% and 50% for $AlPO_4$-5 and $AlPO_4$-11 respectively. These results are surprising. Lachet et al. (1999) and Mohanty et al. (2000) found that whatever the gas composition, the FAU zeolite (KY) and the MFI zeolite (silicalite) were always *para*-selective. In the case of aluminophosphates, the *o*-selectivity appears when the molar fraction of *p*-xylene increases in the mixture. The $\alpha_{px/ox}$ value for the 80% *p*-xylene–20% *o*-xylene mixture was in agreement with experimental results of Rosenfeld and Barthomeuf (1983). Using liquid phase mixtures of C8 aromatics with 25% of *o*-xylene at ambient temperatures, the authors found an $\alpha_{px/ox}$ value of 0.2 (our value for 20% *o*-xylene was 0.24).

Figure 5 shows the gas composition *vs.* the adsorbed phase composition at high loadings for both aluminophosphates. The three simulated points correspond to the three mixtures studied (20% *p*-xylene-80% *o*-xylene, 50% *p*-xylene-50% *o*-xylene and 80% *p*-xylene-20% *o*-xylene). An experimental data point from Rosenfeld and Barthomeuf (1983) for $AlPO_4$-5 is also shown for comparison with our simulation results.

3.3 Azeotropic behaviour

The behavior of the isomers mixture in aluminophosphates pores can be explained if we use the two patches theory proposed by Do and Do (1999). In this theory, the adsorbed phase is considered to be composed of two patches of adsorption sites independent of each other. In our case, the two

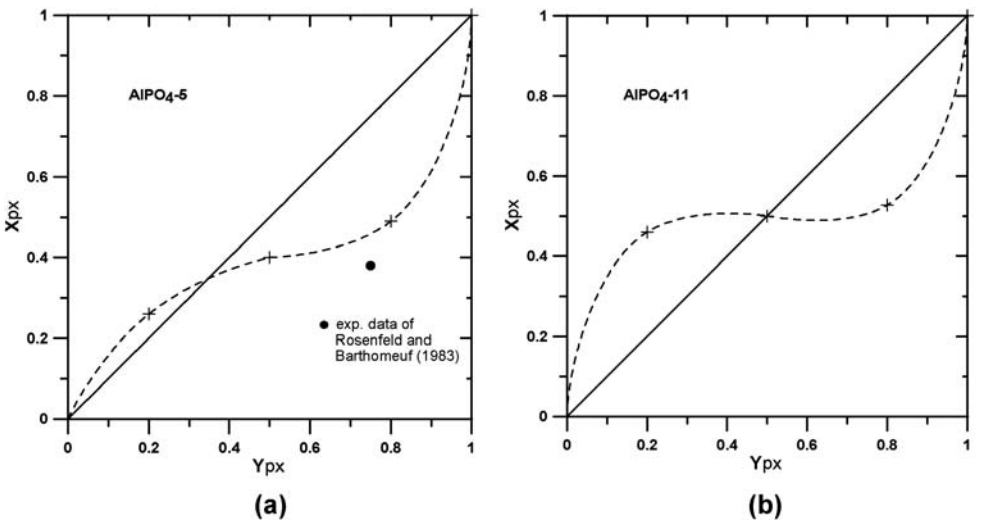

Fig. 5 Simulation results for binary *o*-xylene/*p*-xylene adsorption in aluminophosphates at high loading. (**a**) $AlPO_4$-5; (**b**) $AlPO_4$-11. *Xpx*: molar fraction of *p*-xylene in the adsorbed phase and *Ypx*: molar fraction of *p*-xylene in the gas phase. Experimental point from Rosenfeld and Barthomeuf (1983) is also shown for $AlPO_4$-5 (*filled circle*)

patches are narrow windows and wide regions. Adsorption on each patch is direct from the gas phase. If we assume that patch 1 has stronger adsorption interaction energy than patch 2, and the solid is exposed to fluid components, the two possibilities that will give rise to an azeotropic behavior are:

Case 1—The adsorption on the weaker patch is restricted to the weaker species.
Case 2—The adsorption on the stronger patch is restricted to the weaker species.

Weaker species is defined by Do and Do (1999) as the molecule with lower affinity for patch 1. The authors applied this theory for the systems iso-butane/ethylene/13X and propane/carbon dioxide/mordenite that were known to exhibit azeotropic behaviour.

3.3.1 $AlPO_4$-5

The AFI network is a nice example of the case 1. Based on the location and adsorption heats of the species (Figs. 4 and 3), we can conclude that the stronger patch is the wide regions and the weaker patch is the narrow windows. The *o*-xylene molecules adsorb in the stronger patch (wide region) and the *p*-xylene weaker species is restricted to the narrow windows (the weaker patch). We should remark here that this observation was made using statistics of mass center location from the binary simulations (Sect. 3.1). The azeotropic behavior occurs because, after *o*-xylene occupies the strong patch, the system pressure is high enough to give the weaker species an opportunity to adsorb in sites that are still available of the second patch (narrow windows). Then selectivity reversal occurs, since the narrow windows are accessible only to *p*-xylene.

3.3.2 $AlPO_4$-11 and minimization studies

We know from the study of the location of adsorbed species (Fig. 4) that AEL network has two patches (narrow windows and wide region). Each isomer adsorbs preferentially in one of these sites (*o*-xylene in narrow windows and *p*-xylene in wide region). Unlike $AlPO_4$-5, in $AlPO_4$-11 the isomers adsorption heats are the same. Then, in order to try to find which is the stronger patch we measure the interaction energy while the xylene molecules goes from narrow windows to wide regions.

To do this, we applied the same methodology of Song et al. (2002). In that study the authors measure the interaction energies between benzene and *p*-xylene molecules and the different adsorption sites (channels and intersection channels) of silicalite. They used energy minimization technique. First, the sorbate molecule was forced to diffuse stepwise along the straight channel axis at steps of 0.2 Å. At each step, the system was reminimized. The minimum energies at each step were then recorded. During the simulations, the framework was assumed to be fixed, whereas all the atoms of the sorbate molecules were flexible. Burchart (Vos Burchart et al. 1992) and DREIDING (Mayo et al. 1990) force fields were used.

In our study, we started loading the $AlPO_4$-11 $3 \times 3 \times 3$ simulation cell structure with one xylene molecule through a canonical ensemble Monte Carlo algorithm at 30 °C. The force fields used in the simulations were Burchart (Vos Burchart et al. 1992) for the molecular sieve and UFF (Rappé et al. 1992) for the molecules. The molecule was then forced to diffuse from wide regions to narrow windows (*p*-xylene) or from narrow windows to wide regions (*o*-xylene). The interaction energy between the molecule and the molecular sieve was recorded. As we expected, the interaction energies of *o*- and *p*-xylene in the more stable position were

the same. The energy difference from the more stable position to the less stable position was also the same. The interaction energy varies from approximately 16.50 kcal/mol to 15.00 kcal/mol giving differences of only 0.5 kcal/mol. This small difference value can be compared with those obtained by Bhide and Yashonath (2000) in a molecular dynamic study. They estimated that the adsorption heat of benzene was 13.8 kcal/mol for the wide regions and 12.2 kcal/mol for narrow windows in $AlPO_4$-5 at 27 °C.

We conclude that the azeotropic behaviour in $AlPO_4$-11 can be explained by the case 1 too, but with some particularities. Unlike $AlPO_4$-5, the species affinities to the specific patches in $AlPO_4$-11 are the same. If we use the molecule-molecule energy interaction criterion to identify the stronger patch, then narrow windows will fulfill this role. In narrow windows the molecule-molecule interaction energy is the double of that for wide regions (see Sect. 3.1). So *o*-xylene molecules adsorb in the stronger patch (narrow windows) and the *p*-xylene species is restricted to the wide regions (the weaker patch). The same azeotropic behavior reasoning applied to the $AlPO_4$-5 can then be applied here too.

4 Conclusions

Molecular simulations of the coadsorption of *o*- and *p*-xylene in AFI and AEL networks have been presented. The simulations were performed using the conventional and energy biased GCMC techniques. Energy minimization calculations in $AlPO_4$-11 adsorption sites were done to help evaluate any interaction energy difference. Simulated adsorption isotherms for the mixtures 20% *p*-xylene-80% *o*-xylene, 50% *p*-xylene-50% *o*-xylene and 80% *p*-xylene-20% *o*-xylene were presented.

Xylene molecules are found to be adsorbed in two sites: narrow windows and wide regions along the aluminophosphate pore. In $AlPO_4$-5 *o*- and *p*-xylene have an adsorption heat difference of 1.2 kcal/mol, while the adsorption heats of the isomers in $AlPO_4$-11 are the same. Energy minimization studies in $AlPO_4$-11 reinforce this finding. The *o*-selectivity predicted by single component isotherms was confirmed by the binary mixture simulations. However, the mixture simulations show an unexpected azeotropic behavior. Azeotropic behavior is observed at *p*-xylene gas phase mol fractions under 37% for $AlPO_4$-5 and under 50% for $AlPO_4$-11. Using the two patch theory proposed by Do and Do (1999) we can explain the azeotropic behavior. The azeotropic behavior in $AlPO_4$-11 is a particular case of that of $AlPO_4$-5 because, unlike $AlPO_4$-5, the species affinities to the specific patches in $AlPO_4$-11 are the same.

Acknowledgements The authors thank CAPES, CNPq and FINEP/CTPETRO (S.M.P. Lucena and C.L. Cavalcante) and the U.S. National Science Foundation (CTS-0507013).

References

Barthomeuf, D., De Mallmann, A.: Adsorption of aromatics in NaY and $AlPO_4$-5. Correlation with the sorbent properties in separations. Ind. Eng. Chem. Res. **29**, 1435–1438 (1990)

Bennett, J.M., Cohen, J.P., Flanigen, E.M., Pluth, J.J., Smith, J.V.: Crystal structure of tetrapropylammonium hydroxide-aluminum phosphate number 5. ACS Symp. Ser. **218**, 109–118 (1983)

Bennett, J.M., Richardson, J.W., Pluth, J.J., Smith, J.V.: Aluminophosphate molecular sieve $AlPO_4$-11: partial refinement from powder data using a pulsed neutron source. Zeolites **7**, 160–162 (1987)

Bhide, S.Y., Yashonath, S.: Structure and dynamics of benzene in one-dimensional channels. J. Phys. Chem. B **104**, 11977–11986 (2000)

Buarque, H.L.B., Chiavone, O., Cavalcante, C.L.: Adsorption equilibria of C-8 aromatic liquid mixtures on Y zeolites using headspace chromatography. Sep. Sci. Technol. **40**, 1817–1834 (2005)

Vos Burchart, E., van Bekkum, H., van de Graaf, B., Vogt, E.T.C.: A consistent molecular mechanics force field for aluminophosphates. J. Chem. Faraday Trans. **88**, 2761–2769 (1992)

Cavalcante Jr., C.L., Azevedo, D.C.S., Souza, I.G., Silva, A.C.M., Alsina, O.L.S., Lima, V.E., Araujo, A.S.: Sorption and diffusion of *p*-xylene and *o*-xylene in aluminophosphate molecular sieve $AlPO_4$-11. Adsorption **6**, 53–59 (2000)

Chempath, S., Low, J.J., Snurr, R.Q.: Molecular modeling of binary liquid-phase adsorption of aromatics in silicalite. AIChE J. **50**, 463–469 (2004)

Chiang, A.S.T., Lee, C.K., Chang, Z.H.: Adsorption and diffusion of aromatics in $AlPO_4$-5. Zeolites **11**, 380–386 (1991)

Clark, L.A., Snurr, R.Q.: Adsorption isotherm sensitivity to small changes in zeolite structure. Chem. Phys. Lett. **308**, 155–159 (1999)

Do, D.D., Do, H.D.: On the azeotropic behaviour of adsorption systems. Adsorption **5**, 319–329 (1999)

Frenkel, D., Smit, B.: Understanding Molecular Simulation. Academic, New York (2002)

Gupta, A., Chempath, S., Sanborn, M.J., Clark, L.A., Snurr, R.Q.: Object-oriented programming paradigms for molecular modeling. Mol. Simul. **29**, 29–46 (2003)

Jorgensen, W.L., Laird, E.R., Nguyen, T.B., Tirado-Rives, J.: Monte Carlo simulations of pure liquid substituted benzene with OPLS potential functions. J. Comput. Chem. **14**, 206–215 (1993)

Kiselev, A.V., Lopatkin, A.A., Shulga, A.A.: Molecular statistical calculation of gas adsorption by silicalite. Zeolites **5**, 261–267 (1985)

Lachet, V., Boutin, A., Tavitian, B., Fuchs, A.H.: Computational study of *p*-xylene/*m*-xylene mixtures adsorbed in NaY zeolite. J. Phys. Chem. B **102**, 9224–9233 (1998)

Lachet, V., Boutin, A., Tavitian, B., Fuchs, A.H.: Molecular simulation of *p*-xylene and *m*-xylene adsorption in Y zeolites. Single components and binary mixtures study. Langmuir **15**, 8678–8685 (1999)

Lachet, V., Buttefey, S., Boutin, A., Fuchs, A.H.: Molecular simulation of adsorption equilibria of xylene isomer mixtures in faujasite zeolites. A study of the cation exchange effect on adsorption selectivity. Phys. Chem. Chem. Phys. **3**, 80–86 (2001)

Lucena, S.M.P., Pereira, J.A.F.R., Cavalcante Jr., C.L.: Orthoselectivity in aluminophosphate molecular sieves: A molecular simulation study. Adsorption **12**, 423–434 (2006a)

Lucena, S.M.P., Pereira, J.A.F.R., Cavalcante Jr., C.L.: Structural analysis and adsorption sites of xylenes in $AlPO_4$-5 and $AlPO_4$-11 using molecular simulation. Microporous Mesoporous Mater. **88**, 135–144 (2006b)

Mayo, S.L., Olafson, B.D., Goddard III, W.A.: DREIDING: a generic force field for molecular simulations. J. Phys. Chem. **94**, 8897–8909 (1990)

Minceva, M., Rodrigues, A.E.: Adsorption of xylenes on faujasite-type zeolite–equilibrium and kinetics in batch adsorber. Chem. Eng. Res. Des. **82**, 667–681 (2004)

Mohanty, S., Davis, H.T., McCormick, A.V.: Shape selective adsorption in atomistic nanopores a study of xylene isomers in silicalite. Chem. Eng. Sci. **55**, 2779–2792 (2000)

Rappé, A.K., Casewit, C.J., Colwell, K.S., Goddard, W.A., Skiff, W.M.: UFF, a full periodic table force for molecular mechanics and molecular dynamics simulations. J. Am. Chem. Soc. **114**, 10024–10035 (1992)

Rosenfeld, D.D., Barthomeuf, D.M.: US Patent, 4,482,776, to Exxon (1983)

Ruthven, D.M.: Principles of Adsorption and Adsorption Processes. Wiley, New York (1984)

Snurr, R.Q., Bell, A.T., Theodorou, D.N.: Prediction of adsorption of aromatic hydrocarbons from Grand Canonical Monte Carlo simulations with biased insertions. J. Phys. Chem. **97**, 13742–13752 (1993)

Song, L., Sun, Z.-L., Rees, L.V.C.: Experimental and molecular simulation studies of adsorption and diffusion of cyclic hydrocarbons in silicalite-1. Microporous Mesoporous Mater. **55**, 31–49 (2002)

Sorption, invoked from Cerius2 v. 4.6, Accelrys Inc, San Diego (2001)